

PAPER

Plasma sprayed Cr_3C_2 -NiCr/fly ash cenosphere coating: cyclic oxidation behavior at elevated temperature

To cite this article: Mrityunjay Doddamani *et al* 2018 *Mater. Res. Express* **5** 126404

View the [article online](#) for updates and enhancements.





IOP | ebooks™

Bringing you innovative digital publishing with leading voices to create your essential collection of books in STEM research.

Start exploring the [collection](#) - download the first chapter of every title for free.



PAPER

Plasma sprayed Cr_3C_2 -NiCr/fly ash cenosphere coating: cyclic oxidation behavior at elevated temperatureRECEIVED
1 July 2018REVISED
6 September 2018ACCEPTED FOR PUBLICATION
17 September 2018PUBLISHED
26 September 2018Mrityunjay Doddamani¹, Mahantayya Mathapati²  and M R Ramesh¹ ¹ Department of Mechanical Engineering, National Institute of Technology Karnataka, Surathkal, India² Department of Mechanical Engineering, KLE College of Engineering and Technology, Chikodi, Karnataka, IndiaE-mail: mahantkm@gmail.com

Keywords: plasma spray, cenospheres, elevated temperature, cyclic oxidation

Abstract

Oxidation is one of the major degradation phenomena observed in components subjected to higher temperatures like in thermal power plants (boiler tubes), steam and gas turbines blades etc. Developing protective coatings for such components mitigate oxidation. In the present study, plasma spray technique is utilized to deposit the Cr_3C_2 -NiCr/Cenospheres coating on MDN 321 steel substrate. Thermo cyclic oxidation test is conducted at 600 °C (20 cycles) on both the coating and MDN 321 steel substrate. The thermogravimetric methodology is employed to estimate the oxidation kinetics. Energy Dispersive Spectroscopy (EDS), x-ray Diffraction (XRD), Scanning Electron Microscope (SEM) and x-ray mapping technique is employed to characterize the oxidized samples. Cr_3C_2 -NiCr/Cenosphere coating displayed lower rate of oxidation as compared to substrate implying its suitability in high-temperature applications. Protective oxides like Al_2O_3 , Cr_2O_3 , and NiCr_2O_4 are observed on the uppermost layer of the coating lowering the oxidation rate in the developed coating.

1. Introduction

Many industrial components like power generation boilers, gas and steam turbine, hot sections of the aero engine working at elevated temperatures, experience oxidation, erosion and hot corrosion leading to reduced life cycle [1–7]. At present, Fe and Ni-based alloys are used for such applications which possess excellent strength and mechanical properties. Nevertheless, these alloys exhibit lower resistance to erosion, oxidation and hot corrosion. These surface properties can be improved by choosing appropriate surface adaption techniques. Thermal spray coating is widely utilized in elevated temperature applications to prevent erosion, oxidation and hot corrosion. The degree of mechanical property retention, when subjected to elevated temperature environments, is observed to be higher in such coatings [8]. Among the available thermal spray coating techniques, plasma spray technique is considered as the most versatile, flexible and cost-effective solution for aforementioned applications [9].

Plasma sprayed Cr_3C_2 -NiCr coatings are widely used to minimize erosion, oxidation, and corrosion in high-temperature applications [10–13]. Carbide particles embedded in NiCr matrix impart high hardness and strength to coatings up to 900 °C [14, 15]. These coatings develop the Cr_2O_3 protective oxide layer when they are exposed to elevated temperature improving oxidation resistance [16]. Jagadeeswaran *et al* [17] evaluated the oxidation behavior of Cr_3C_2 /NiCrAlY coating deposited using HVOF technique and found that the coating has better resistance to oxidation at 800 °C as compared to Ti alloy. Kaur *et al* [18] showed the excellent resistance of Cr_3C_2 -NiCr coating (HVOF) to hot corrosion and oxidation as compared to SAE-347H substrate owing to Cr_2O_3 oxide layer formation on the coating surface. However, Cr_3C_2 -NiCr coating feedstock is quite expensive limiting its wide adaptability in the different industrial application. This fact demands the development of inexpensive coating compositions. The probable alternative can be the incorporation of abundantly available industrial waste such as fly ash microspheres.

Fly ash is an abundantly available industrial by-product from thermal power plants, produced by combustion of coal [19]. Fly ash consists of hollow particles called cenospheres [20, 21]. These cenospheres are

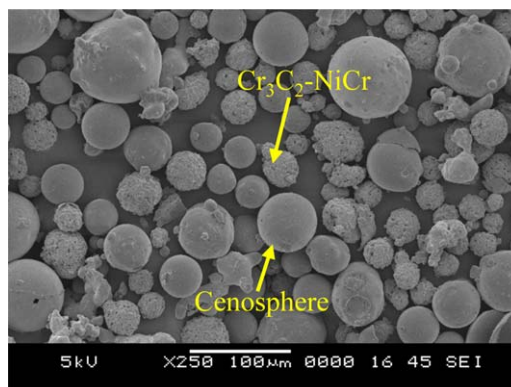


Figure 1. As blended $\text{Cr}_3\text{C}_2\text{-NiCr/Cenosphere}$ powder morphology.

Table 1. Powders particle size distribution.

Size (μm)	$\text{Cr}_3\text{C}_2\text{-NiCr}$	Cenospheres ^a
D(0.1)	26.91	—
D(0.5)	46.49	—
D(0.9)	79.31	—
0%–10%	—	106
70%–90%	—	63
0%–30%	—	53
Mean	50.35	65.00

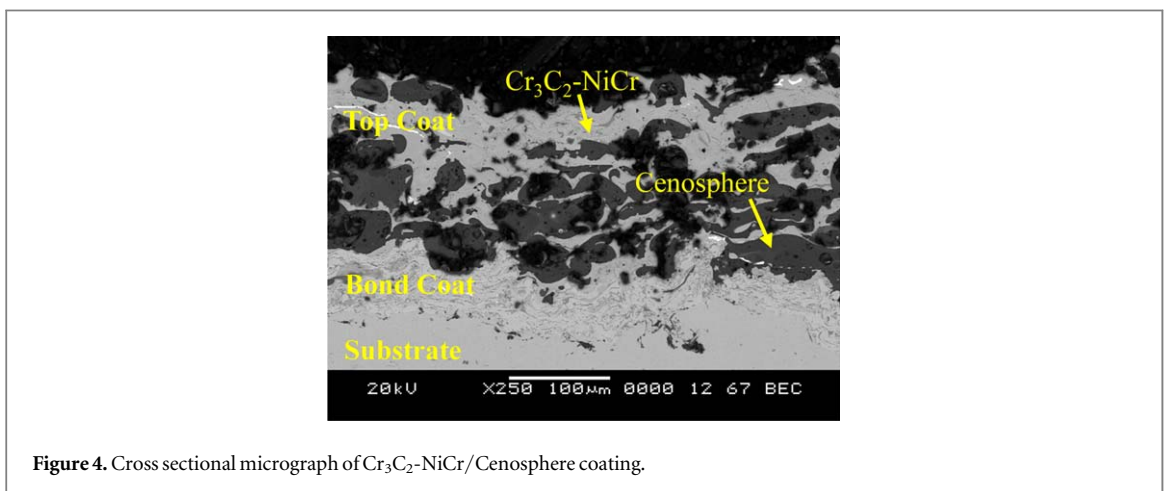
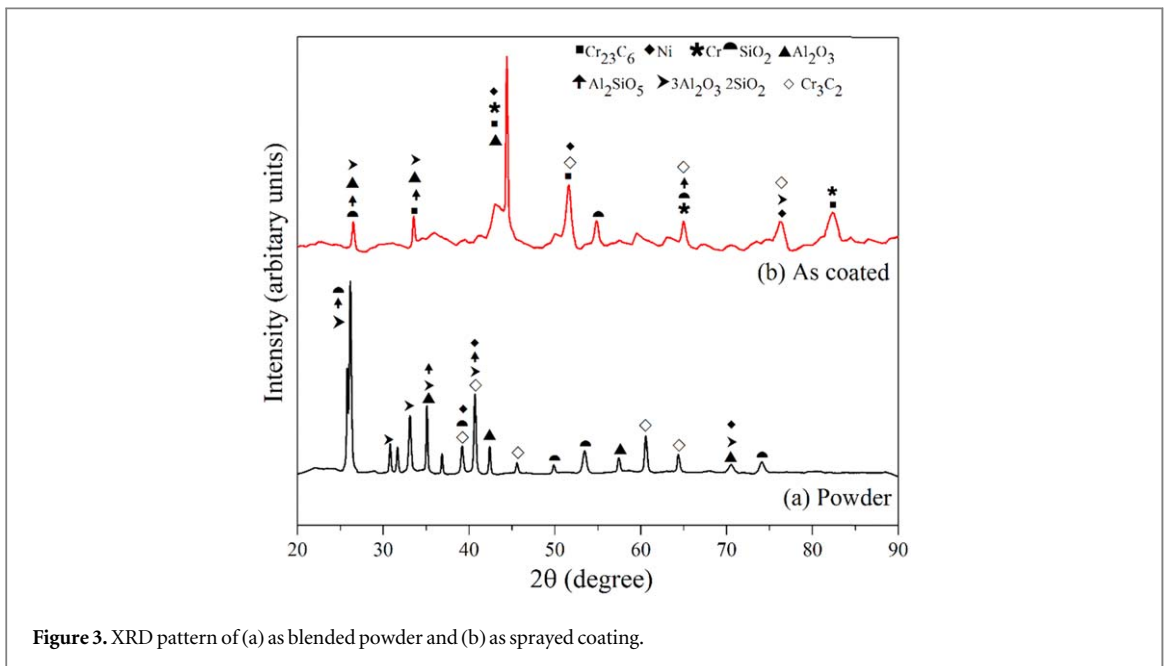
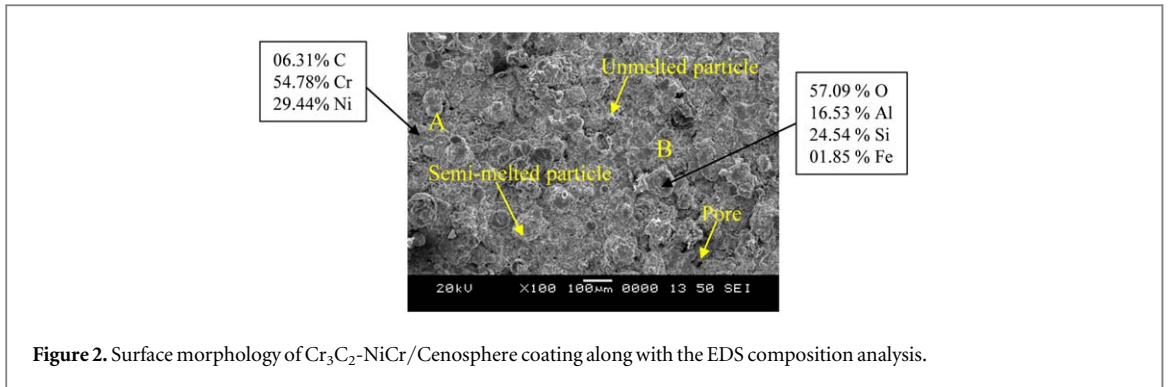
^a As specified by Cenosphere India Pvt. Ltd, Kolkata, India.

Table 2. Process parameters [13]^a.

Argon	Pressure (MPa)	0.75
	Flow (lpm)	40
Hydrogen	Pressure (MPa)	0.35
	Flow (lpm)	7
Current (A)		490
Voltage (V)		60
Powder feed rate (g/min)		60
Stand of distance (mm)		100–125

^a As provided by Spraymet Surface Technology Pvt. Ltd.

spherical in shape, cheaper and exhibit an excellent mechanical response, making them suitable feedstock for thermal spray coatings [22–25]. Fly ash cenospheres constitute SiO_2 , Al_2O_3 and $3\text{Al}_2\text{O}_3 \cdot 2\text{SiO}_2$ [26–29]. Al_2O_3 and $3\text{Al}_2\text{O}_3 \cdot 2\text{SiO}_2$ exhibit stability at elevated temperatures, wear, oxidation resistance etc [30, 31]. Many researchers have presented the viability of fly ash coating as feedstock and they reported that fly ash can be utilized in plasma spray coatings techniques as coating feedstock [32, 33]. Arizmendi-Morquecho *et al* [30] developed the thermal barrier cenosphere coatings for high-temperature applications. They studied the thermal conductivity and coefficient of thermal expansion of the coating at 1200 K and reported that the coating exhibits low thermal conductivity ($0.17 \text{ W m}^{-1} \text{ K}^{-1}$) and low thermal expansion coefficient (5.96×10^{-6}) making it suitable for elevated temperature applications. Sidhu *et al* [34] developed a fly ash coating on carbon steel using a plasma spray technique and revealed better salt corrosion and oxidation resistance in comparison with the substrate. However, the literature on higher temperature oxidation resistance of fly ash cenospheres composite coatings is relatively scarce. This fact demands the investigation of high-temperature oxidation response of composite coating comprising of $\text{Cr}_3\text{C}_2\text{-25NiCr}$ and cenospheres. Furthermore, development of such cenospheres coatings lower the disposal linked issues effectively.



In the present study, Cr_3C_2 -25NiCr/Cenosphere coating is developed by a plasma spray technique on MDN 321 steel substrate. Cyclic oxidation response of MDN 321 steel and coating is investigated at 600 °C in air for 20 cycles and results are presented for analysis.

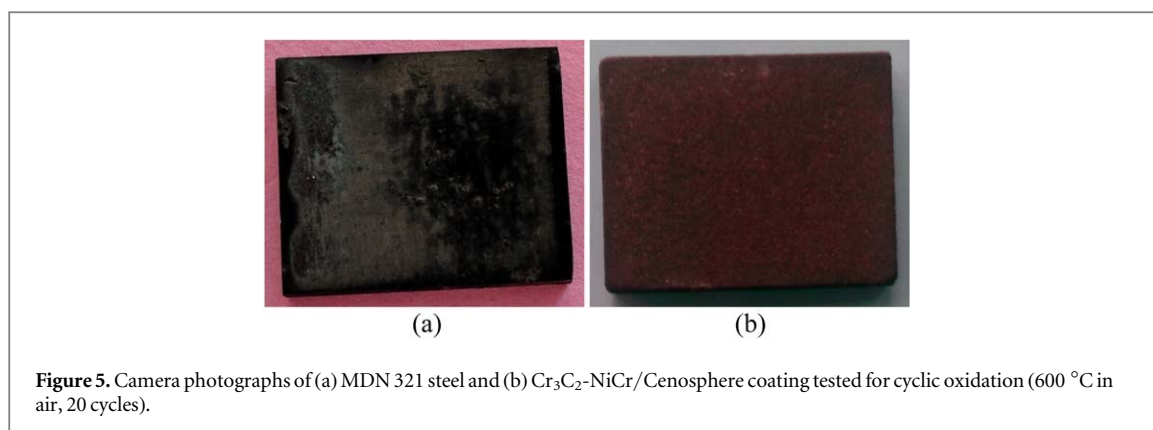


Figure 5. Camera photographs of (a) MDN 321 steel and (b) Cr₃C₂-NiCr/Cenosphere coating tested for cyclic oxidation (600 °C in air, 20 cycles).

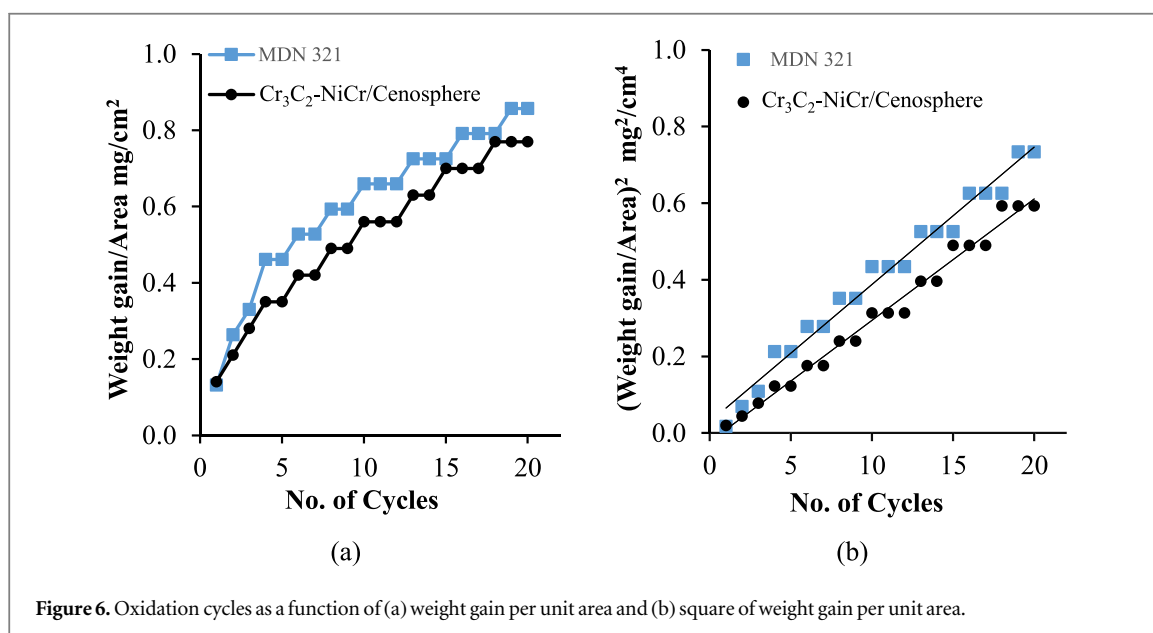


Figure 6. Oxidation cycles as a function of (a) weight gain per unit area and (b) square of weight gain per unit area.

2. Materials and methods

2.1. Materials

MDN 321 steel is utilized as substrate (Mishra Dhatu Nigam Ltd, Hyderabad, India) having a chemical composition of Fe-0.1C-1.46Mn-18.13Cr-10.36Ni-0.62Ti-0.55Si (wt%). The samples of 25 × 20 × 4 mm dimension are used for plasma spraying. Commercially available agglomerated and sintered Cr₃C₂-25NiCr powder (Praxair 1375 VM C⁻¹R⁻¹C⁻¹-300-1, USA) and cenospheres (Cenospheres India Pvt. Ltd, Kolkata, India) are used as coatings feedstock. The density of the Cr₃C₂-25NiCr powder and cenosphere are 2.6 and 0.85 g cm⁻³ respectively. The laser diffraction technique (Cilas, 1064, France) is employed to calculate the nominal mean particle size distribution of the Cr₃C₂-25NiCr powder and the results are detailed in table 1. Cr₃C₂-25NiCr and fly ash cenospheres powders are blended mechanically with 70:30 weight fraction prior to plasma spraying. Figure 1 demonstrates the SEM micrograph of as blended composition. It is observed from the figure 1 that cenospheres are uniformly distributed in Cr₃C₂-25NiCr network indicating the viability of the method used for blending.

2.2. Coating deposition and characterization

METCO USA 3MB plasma spray gun (Spraymet Surface Technologies Pvt. Ltd, Bangalore) is employed to spray the Cr₃C₂-NiCr/Cenosphere blend. Prior to spraying, the surface of the substrates is roughened by grit blasting using alumina powder of 150 μm size. Argon is utilized as powder carrier gas while hydrogen is used as a plasma generating gas. Table 2 lists the used spray parameters. Prior to plasma coating, blended powder of Cr₃C₂-25NiCr and cenosphere is supplied to the feeder through the hopper. Further, powder from the feeder gets mixed with the argon gas at a chosen pressure and move towards the plasma stream to get a deposit on the substrate [13]. Before depositing the Cr₃C₂-NiCr/Cenosphere coating, NiCr bond coat is sprayed on the

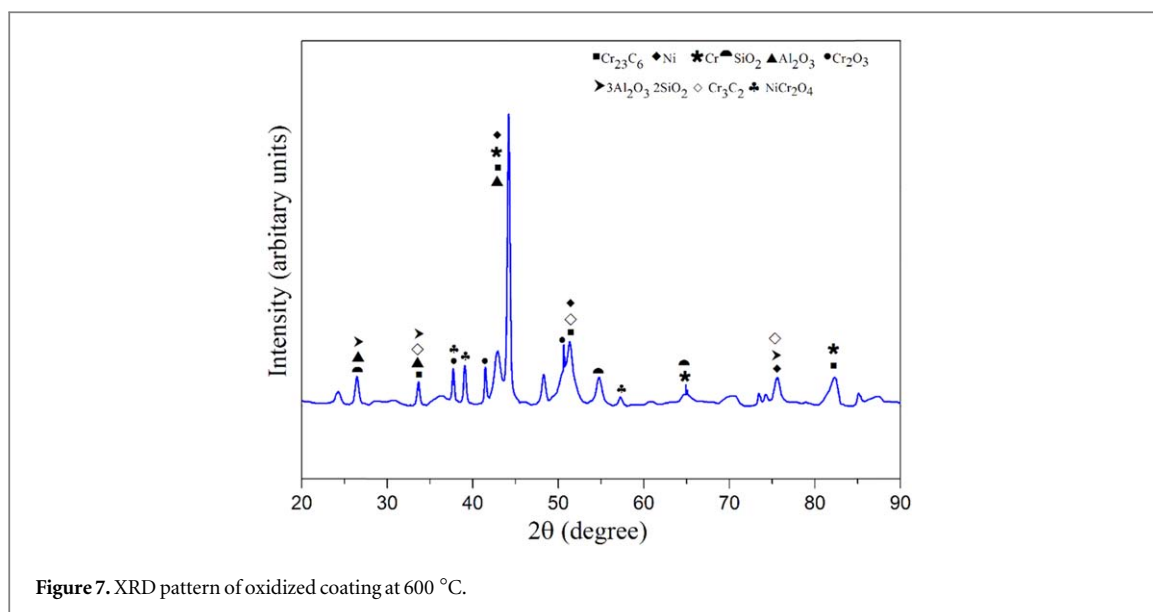


Figure 7. XRD pattern of oxidized coating at 600 °C.

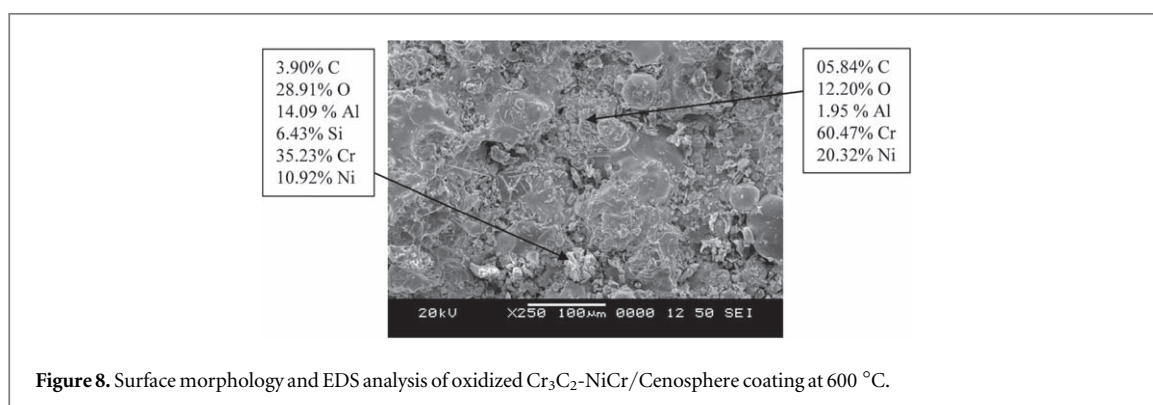


Figure 8. Surface morphology and EDS analysis of oxidized Cr_3C_2 -NiCr/Cenosphere coating at 600 °C.

substrate to enhance the adhesion strength of the coating. After spraying, samples are cut, cold mounted and polished with emery papers and cloth to get the mirror finish. Surface morphology and coating thickness are observed using SEM. Phases in blended powder, as sprayed and oxidized coating is analyzed using XRD (DX GE-2P, Jeol, Japan). EDS is utilized to analyze the elemental composition of the coating.

2.3. Cyclic oxidation test

Heatron Industrial Heaters, Mangalore make furnace (tubular) is used to carry out the cyclic oxidation test on the substrate as well as on the coated samples for 20 cycles at 600 °C. Each cycle consists of 1 h of 600 °C heating followed by ambient temperature cooling for 20 min. The surface area of the substrate and the coated samples are calculated using a vernier caliper prior to the test. Weight change is recorded for each cycle by electronic balance having a sensitivity of 0.01 mg. Cyclic oxidation is chosen to simulate actual conditions in the thermal power plant (frequent power failures).

3. Results and discussion

3.1. Coating surface morphology and XRD analysis

Cr_3C_2 -NiCr/Cenosphere coating as sprayed surface morphology and EDS analysis at selected points are presented in figure 2. Surface morphology of the as-sprayed coating consists of a melted matrix, semi-melted particles, few intact particles, and pores. The pores are formed during solidification and due to the fracture of cenospheres during splat formation. EDS point analysis at point A is rich in chromium and nickel representing the matrix region. Point B is rich in aluminum and silicon indicating cenosphere particle.

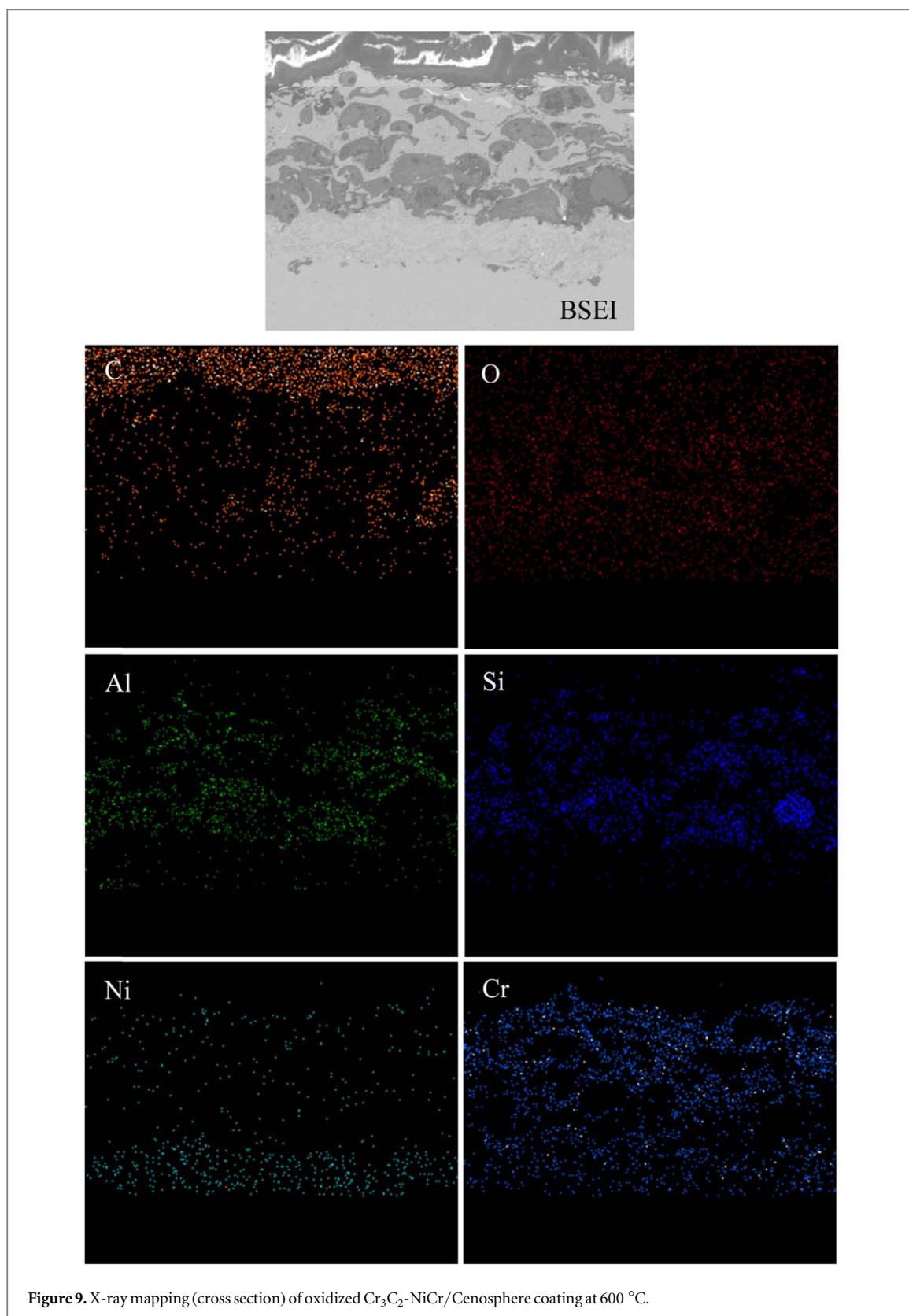


Figure 3 demonstrates the XRD result of as blended powder and coating depicting $3\text{Al}_2\text{O}_3 \cdot 2\text{SiO}_2$, Al_2SiO_5 , SiO_2 (major phases) and Cr_3C_2 , Al_2O_3 (minor phases). XRD of an as-sprayed coating composed of Cr_{23}C_6 , Cr, Al_2O_3 and Ni (major phase) and SiO_2 , Al_2SiO_5 (minor phases).

3.2. Microstructure analysis

Cr_3C_2 -NiCr/Cenosphere coating cross sectional microstructure is exhibited by figure 4. NiCr bond coat adheres well to the substrate and coating as seen in figure 4. Thickness (average) of the bond coat and the coating is 50 and

200 μm respectively. Coating constituents, cenospheres (dark gray phase) are distributed uniformly in the $\text{Cr}_3\text{C}_2\text{-NiCr}$ (light gray phase) with fully melted splats and some semi-melted particles, which are bonded together as noticed from figure 4.

3.3. Visual observations of oxidized samples

The camera photographs of the MDN 321 steel substrate and $\text{Cr}_3\text{C}_2\text{-NiCr}$ /cenosphere coating after cyclic oxidation in air at 600 $^\circ\text{C}$ for 20 cycles are presented in figure 5. At the end of the oxidation cycles, no spalling is observed for both MDN 321 steel and coating, while dark brown color oxide scale is noticed on the surface of $\text{Cr}_3\text{C}_2\text{-NiCr}$ /Cenosphere coating. Post 20 cycles, the coating is seen to be in good contact with the substrate. The oxide scale is found to be compact, smooth with the absence of cracks.

3.4. Thermo gravimetric behavior

Cumulative weight gain plots and weight gain square as a function of a number of cycles of MDN 321 steel and $\text{Cr}_3\text{C}_2\text{-NiCr}$ /Cenosphere coating are presented in figures 6(a) and (b) respectively. It is observed that, both substrate and coating experience rapid increments in the weight gain in the initial 5 cycles and gradual increment in weight gain for the remaining cycles. The weight gain post 20 cycles for MDN 321 steel substrate and $\text{Cr}_3\text{C}_2\text{-NiCr}$ /Cenosphere coating is 0.85 and 0.77 mg cm^{-2} respectively. $\text{Cr}_3\text{C}_2\text{-NiCr}$ /Cenosphere coatings resulted in lower weight gain as compared to MDN 321 owing to the formation of a protective oxide layer on the surface. Figure 6(b) depicts the plot of weight gain square against a number of cycles. The oxidation behavior of MDN 321 steel, as well as coating, is parabolic in nature up to 20 cycles. Kinetics of oxidation is approximated by the parabolic rate law. The parabolic rate constant [35] is calculated using the linear least square fit method as,

$$\left(\frac{dW}{A}\right)^2 = K_p \times t \quad (1)$$

where, $\frac{dW}{A}$ is the weight gain per unit area, t is the oxidized time in seconds. The parabolic rate constants (K_p in $10^{-10} \text{ g}^2 \text{ cm}^{-4} \text{ s}^{-1}$) for MDN 321 steel and $\text{Cr}_3\text{C}_2\text{-NiCr}$ /Cenosphere coating is 0.099 and 0.0317 respectively.

3.5. XRD and EDS analysis of oxidized coating

Figure 7 shows the XRD pattern of coating oxidized at 600 $^\circ\text{C}$. In oxidized coating Cr_{23}C_6 , Al_2O_3 , Cr, and Ni are found as a major phase while SiO_2 is found as a minor phase. Cr_2O_3 and NiCr_2O_4 oxides are observed in the XRD pattern as a result of oxidation. These oxides form the protective oxide scale on the surface of the coating thereby protects the coating [18].

The oxidized surface microstructure of the $\text{Cr}_3\text{C}_2\text{-NiCr}$ /Cenosphere coating along with EDS result is presented in figure 8. Oxide scale mainly consists of Ni, Cr, Al, Si, and O suggesting the formation of Ni, Cr, Al, and Si oxides (figure 8). XRD result of coating which is undergone oxidation also confirms the presence of Al_2O_3 , Cr_2O_3 and SiO_2 oxides on the coating surface. Al_2O_3 and SiO_2 oxides are formed mainly due to the presence of cenospheres in the coating, as cenospheres are rich in Al_2O_3 and SiO_2 . These Al_2O_3 and SiO_2 oxides improve the oxidation resistance of the coating and lower the scale spallation as suggested by Sidhu *et al* [34]. Presence of $\text{Cr}_3\text{C}_2\text{-NiCr}$ in the coating contributes to the formation of Cr_2O_3 and NiCr_2O_4 oxides on the coating surface. Therefore, the synergetic effect of $\text{Cr}_3\text{C}_2\text{-NiCr}$ and cenospheres increases the oxidation resistance of the $\text{Cr}_3\text{C}_2\text{-NiCr}$ /Cenosphere coating.

Cross-sectional elemental x-ray mapping of $\text{Cr}_3\text{C}_2\text{-NiCr}$ /Cenosphere coating which is undergone cyclic oxidation for 20 cycles is depicted by figure 9. X-ray mapping revealed that the topmost layer is rich in Cr, Ni, Al, and O indicating Al_2O_3 , Cr_2O_3 , and NiCr_2O_4 oxide formation. The oxide scale established on the top layer prevents the inward diffusion of oxygen and other oxidizing elements into the coating [36].

4. Conclusion

- Plasma spray technique has been successfully utilized to develop $\text{Cr}_3\text{C}_2\text{-NiCr}$ /Cenosphere coating on MDN 321 steel with an average thickness of 200 μm .
- The coating exhibited higher resistance to oxidation compared to MDN 321 steel at 600 $^\circ\text{C}$. Coating weight gain is noted to be 9.41% lower than the MDN 321 steel.
- Better oxidation performance of the coating is attributed to Al_2O_3 , SiO_2 , Cr_2O_3 and NiCr_2O_4 oxides formed on the coating surface.
- The formed oxides act as a diffusion barrier for oxygen and control the penetration of oxygen into the coating.

Acknowledgments

The authors wish to thank Spraymet Surface technologies Pvt Ltd, Bangalore, India, for providing the facility of the plasma spray coating. All the authors thank the Mechanical Engineering department at NITK Surathkal for providing support in carrying out this work. This research did not receive any specific grant from funding agencies in the public, commercial, or not-for-profit sectors.

ORCID iDs

Mahantayya Mathapati  <https://orcid.org/0000-0002-5436-7815>

M R Ramesh  <https://orcid.org/0000-0003-4302-2958>

References

- [1] Zhou W, Zhou K, Deng C, Zeng K and Li Y 2017 Hot corrosion behavior of HVOF-sprayed Cr₃C₂-WC-NiCoCrMo coating *Ceram. Int.* **43** 9390–400
- [2] Singh H, Kaur M and Prakash S 2016 High-temperature exposure studies of HVOF-sprayed Cr₃C₂-25 (NiCr)/(WC-Co) coating *J. Therm. Spray Technol.* **25** 1192–207
- [3] Ramesh M, Prakash S, Nath S, Sapra P K and Venkataraman B 2010 Solid particle erosion of HVOF sprayed WC-Co/NiCrFeSiB coatings *Wear* **269** 197–205
- [4] Jafari M, Enayati M, Salehi M, Nahvi S, Han J and Park C 2016 High temperature oxidation behavior of micro/nanostructured WC-Co coatings deposited from Ni-coated powders using high velocity oxygen fuel spraying *Surf. Coat. Technol.* **302** 426–37
- [5] Prasad C D, Joladarashi S, Ramesh M, Srinath M and Channabasappa B 2018 Influence of microwave hybrid heating on the sliding wear behaviour of HVOF sprayed CoMoCrSi coating *Mater. Res. Express* **5** 086519
- [6] Nithin H S, Desai V and Ramesh M 2018 Elevated temperature solid particle erosion behaviour of carbide reinforced CoCrAlY composite coatings *Mater. Res. Express* **5** 066529
- [7] Chen K, Song P, Hua C, Zhou Y, Huang T, Li C and Lu J 2018 Effect of YSZ-dopant on microstructure and hardness property of the Al₂O₃-40% TiO₂ plasma sprayed coating *Mater. Res. Express* **5** 086504
- [8] Eriksson R, Yuan K, Li X-H and Peng R L 2015 Corrosion of NiCoCrAlY coatings and TBC systems subjected to water vapor and sodium sulfate *J. Therm. Spray Technol.* **24** 953–64
- [9] Fauchais P 2004 Understanding plasma spraying *J. Phys. D: Appl. Phys.* **37** R86
- [10] Li S-Q, Li Q-L, Gong S-L and Wang C 2011 Researching for corrosion-resistance performance of laser-hybrid plasma spraying NiCr-Cr₃C₂ coating *Physics Procedia* **18** 211–5
- [11] Sreenivasulu V and Manikandan M 2018 High-temperature corrosion behaviour of air plasma sprayed Cr₃C₂-25NiCr and NiCrMoNb powder coating on alloy 80A at 900 °C *Surf. Coat. Technol.* **337** 250–9
- [12] Lin L, Li G-L, Wang H-D, Kang J-J, Xu Z-L and Wang H-J 2015 Structure and wear behavior of NiCr-Cr₃C₂ coatings sprayed by supersonic plasma spraying and high velocity oxy-fuel technologies *Appl. Surf. Sci.* **356** 383–90
- [13] Mathapati M, Ramesh M and Doddamani M 2017 High temperature erosion behavior of plasma sprayed NiCrAlY/WC-Co/cenosphere coating *Surf. Coat. Technol.* **325** 98–106
- [14] Yang G-J, Li C-J, Zhang S-J and Li C-X 2008 High-temperature erosion of HVOF sprayed Cr₃C₂-NiCr coating and mild steel for boiler tubes *J. Therm. Spray Technol.* **17** 782–7
- [15] Manjunatha M, Kulkarni R and Krishna M 2014 Investigation of HVOF thermal sprayed Cr₃C₂-NiCr cermet carbide coatings on erosive performance of AISI 316 molybdenum steel *Procedia Materials Science* **5** 622–9
- [16] Ghosh D and Mitra S 2015 Plasma sprayed Cr₃C₂-Ni-Cr coating for oxidation protection of 2 · 25Cr-1Mo steel *Surf. Eng.* **31** 342–8
- [17] Jegadeeswaran N, Ramesh M and Bhat K U 2014 Oxidation resistance HVOF sprayed coating 25%(Cr₃C₂-25 (Ni₂₀Cr))+ 75% NiCrAlY on titanium alloy *Procedia Materials Science* **5** 11–20
- [18] Kaur M, Singh H and Prakash S 2009 High-temperature corrosion studies of HVOF-sprayed Cr₃C₂-NiCr coating on SAE-347H boiler steel *J. Therm. Spray Technol.* **18** 619
- [19] Doddamani M and Kulkarni S M 2011 Dynamic response of fly ash reinforced functionally graded rubber composite sandwiches - a Taguchi approach *International Journal of Engineering, Science and Technology* **3** 17
- [20] Doddamani M, Kulkarni S M and Kishore 2011 Behavior of sandwich beams with functionally graded rubber core in three point bending *Polym. Compos.* **32** 1541–51
- [21] Jayavardhan M L, Bharath Kumar B R, Doddamani M, Singh A K, Zeltmann S E and Gupta N 2017 Development of glass microballoon/HDPE syntactic foams by compression molding *Composites Part B: Engineering* **130** 119–31
- [22] Manakari V, Parande G, Doddamani M, Gaitonde V, Siddhalingshwar I, Shunmugasamy V C and Gupta N 2015 Dry sliding wear of epoxy/cenosphere syntactic foams *Tribol. Int.* **92** 425–38
- [23] Bharath Kumar B R, Doddamani M, Zeltmann S E, Gupta N, Ramesh M R and Ramakrishna S 2016 Processing of cenosphere/HDPE syntactic foams using an industrial scale polymer injection molding machine *Mater. Des.* **92** 414–23
- [24] Zeltmann S E, Bharath Kumar B R, Doddamani M and Gupta N 2016 Prediction of strain rate sensitivity of high density polyethylene using integral transform of dynamic mechanical analysis data *Polymer* **101** 1–6
- [25] Bharath Kumar B R, Doddamani M, Zeltmann S E, Gupta N, Uzma, Gurupadu S and Sailaja R R N 2016 Effect of particle surface treatment and blending method on flexural properties of injection-molded cenosphere/HDPE syntactic foams *J. Mater. Sci.* **51** 3793–805
- [26] Kumar B B, Singh A K, Doddamani M, Luong D D and Gupta N 2016 Quasi-static and high strain rate compressive response of injection-molded cenosphere/HDPE syntactic foam *JOM* **68** 1861–71
- [27] Kumar B B, Doddamani M, Zeltmann S E, Gupta N and Ramakrishna S 2016 Data characterizing tensile behavior of cenosphere/HDPE syntactic foam *Data in Brief* **6** 933–41
- [28] Doddamani M, Shunmugasamy V C, Gupta N and Vijayakumar H 2015 Compressive and flexural properties of functionally graded fly ash cenosphere-epoxy resin syntactic foams *Polym. Compos.* **36** 685–93

- [29] Bharath Kumar B R, Zeltmann S E, Doddamani M, Gupta N, Uzma, Gurupadu S and Sailaja R R N 2016 Effect of cenosphere surface treatment and blending method on the tensile properties of thermoplastic matrix syntactic foams *J. Appl. Polym. Sci.* **133** 43881
- [30] Arizmendi-Morquecho A, Chávez-Valdez A and Alvarez-Quintana J 2012 High temperature thermal barrier coatings from recycled fly ash cenospheres *Appl. Therm. Eng.* **48** 117–21
- [31] Das S, Ghosh S, Pandit A, Bandyopadhyay T, Chattopadhyay A and Das K 2005 Processing and characterisation of plasma sprayed zirconia–alumina–mullite composite coating on a mild-steel substrate *J. Mater. Sci.* **40** 5087–9
- [32] Mishra S, Rout K, Padmanabhan P and Mills B 2000 Plasma spray coating of fly ash pre-mixed with aluminium powder deposited on metal substrates *J. Mater. Process. Technol.* **102** 9–13
- [33] Muhammad M, Jalar A, Shamsudin R and Isa M 2014 Effect of plasma spray parameters on porosity of fly ash deposited coatings *AIP Conf. Proc. (New York)* (AIP)
- [34] Sidhu B S, Singh H, Puri D and Prakash S 2007 Wear and oxidation behaviour of shrouded plasma sprayed fly ash coatings *Tribol. Int.* **40** 800–8
- [35] Sahu S P, Satapathy A, Patnaik A, Sreekumar K and Ananthapadmanabhan P 2010 Development, characterization and erosion wear response of plasma sprayed fly ash–aluminum coatings *Mater. Des.* **31** 1165–73
- [36] Somasundaram B, Kadoli R and Ramesh M 2014 Evaluation of cyclic oxidation and hot corrosion behavior of HVOF-sprayed WC-Co/NiCrAlY coating *J. Therm. Spray Technol.* **23** 1000–8